

Catalysis Science & Technology

Accepted Manuscript



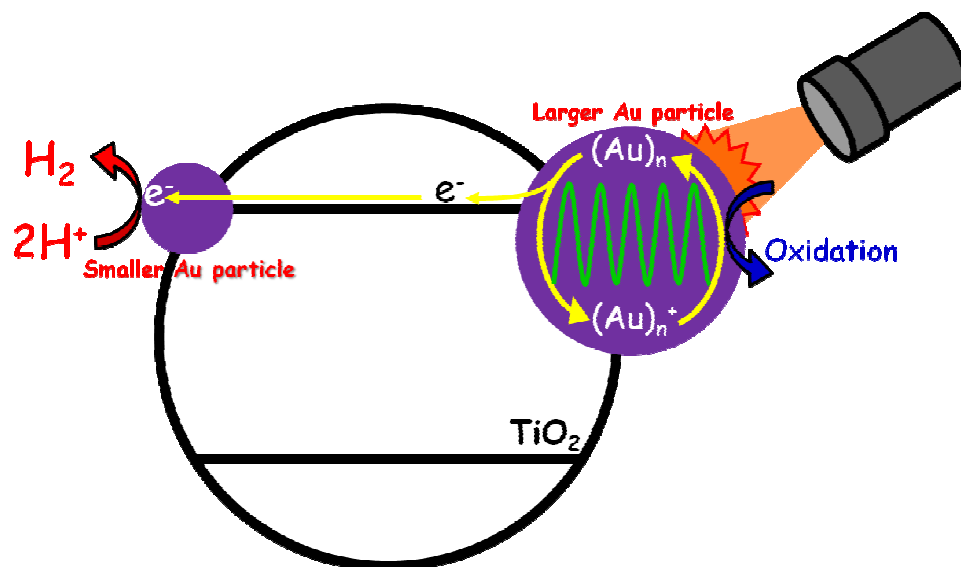
This is an *Accepted Manuscript*, which has been through the Royal Society of Chemistry peer review process and has been accepted for publication.

Accepted Manuscripts are published online shortly after acceptance, before technical editing, formatting and proof reading. Using this free service, authors can make their results available to the community, in citable form, before we publish the edited article. We will replace this *Accepted Manuscript* with the edited and formatted *Advance Article* as soon as it is available.

You can find more information about *Accepted Manuscripts* in the [Information for Authors](#).

Please note that technical editing may introduce minor changes to the text and/or graphics, which may alter content. The journal's standard [Terms & Conditions](#) and the [Ethical guidelines](#) still apply. In no event shall the Royal Society of Chemistry be held responsible for any errors or omissions in this *Accepted Manuscript* or any consequences arising from the use of any information it contains.

TiO₂ having both smaller and larger Au particles exhibited H₂ formation rate larger than that of sample without smaller particles.



Cite this: DOI: 10.1039/c0xx00000x

www.rsc.org/xxxxxx

Photocatalytic reactions under irradiation of visible light over gold nanoparticles supported on titanium(IV) oxide powder prepared by using multi-step photodeposition method

Atsuhiko Tanaka, Satoshi Sakaguchi, Keiji Hashimoto and Hiroshi Kominami*

Received (in XXX, XXX) Xth XXXXXXXXXX 20XX, Accepted Xth XXXXXXXXXX 20XX

DOI: 10.1039/b000000x

Titanium(IV) oxide (TiO₂) having both smaller and larger gold (Au) particles was successfully prepared by the multi-step (MS) photodeposition method. When 0.25 wt% Au loading per photodeposition was repeated four times, smaller and larger Au particles having average diameters of 1.4 and 13 nm, respectively, were fixed on TiO₂, and the Au/TiO₂ sample exhibited strong photoabsorption around 550 nm due to surface plasmon resonance (SPR) of the larger Au particles. Various Au/TiO₂ samples were prepared by changing the Au loading per photodeposition and the number of photodepositions. Effects of the conditions in MS photodeposition and sample calcination on Au particle distribution and photoabsorption properties were investigated. These samples were used for hydrogen (H₂) formation from 2-propanol and mineralization of acetic acid in aqueous suspensions under irradiation of visible light. In the case of H₂ formation under deaerated conditions, the reaction rate of Au/TiO₂ having both larger and smaller particles was 4-times larger than that of the Au/TiO₂ sample without smaller Au particles, indicating that smaller Au particles acted effectively as a co-catalyst, that is, as reduction sites for H₂ evolution. On the other hand, in the case of mineralization of acetic acid under aerated conditions, carbon dioxide formation rates were independent of the presence of smaller Au particles, indicating that the smaller Au particles had little effect on the mineralization of acetic acid. To extend the possibility of Au/TiO₂ for H₂ formation under irradiation of visible light, H₂ formation from ammonia (NH₃) as biomass waste was examined under deaerated conditions, and NH₃ was decomposed to H₂ and nitrogen with a stoichiometric ratio (3:1).

Introduction

Various reactions including oxidation of organic compounds,¹ reduction of aromatic compounds² and hydrogen (H₂) production³ by semiconductor photocatalysts such as titanium(IV) oxide (TiO₂) have attracted much attention. In the case of H₂ production, TiO₂ represents a promising technology to use renewable resources for clean and environmentally friendly energy production. TiO₂ is a wide band gap photocatalyst (band gap = 3.2 eV) that can induce evolution of H₂ from various compounds under ultraviolet (UV) light irradiation.¹⁻³ However, UV light accounts for only about 5% of total solar energy, while visible light accounts for about 50% of total solar energy. Therefore, the development of photocatalysts using visible light is an important topic from a practical point of view.

Modification of TiO₂ photocatalysts has often been used to extend their absorption wavelength from the UV region to visible region. To the best of our knowledge, these photocatalysts can be roughly classified into two types. The first type is TiO₂ doped with nitrogen⁴ and sulfur⁵ as bulk modifiers. The energy levels of nitrogen and sulfur were inserted in the forbidden band of TiO₂, resulting in response to visible light. The second type is semiconductors modified with metal ions such as copper ions (Cu²⁺) utilizing interface charge transfer (IFCT)⁶ and TiO₂ samples modified with an inorganic sensitizer such as platinum(IV) and rhodium(III) chlorides.⁷

Unique optical properties of gold (Au) nanoparticles have been applied in many fields including biochemistry, sensing science, and catalysis.⁸ Nanoparticles of Au show strong photoabsorption of visible light at around ca. 550 nm due to surface plasmon resonance (SPR). SPR of Au nanoparticles has been applied to a visible light-responding photocatalyst.^{9, 10, 11} These photocatalysts have been widely used for SPR-induced photoabsorption in chemical reactions, i.e., oxidation of organic substrates,^{10d-e, 11a-c, 11g} selective oxidation of aromatic alcohol to a carbonyl compound,^{10c, 11d, 11f} H₂ formation from alcohols,^{10f-g, 11e, 11h} dioxygen (O₂) formation from water in the presence of hexavalent chromium as an electron scavenger^{11k} and selective reduction of organic compounds.^{10h, 11j} In our previous communication,^{11e} we described a multi-step (MS) photodeposition method for preparation of Au/TiO₂ samples, in which photodeposition of Au was divided into several steps; for example, photodeposition of 0.25 wt% Au was repeated four times to obtain a 1.00 wt% Au/TiO₂ sample. We reported that Au/TiO₂ samples prepared by the MS photodeposition method (MS-Au/TiO₂) exhibited stronger photoabsorption at around 550 nm due to SPR and higher levels of activity for H₂ production under irradiation of visible light. Since MS-Au/TiO₂ samples exhibited a unique bimodal distribution of Au particles, we suggested that functions of Au/TiO₂ could be shared by Au particles with different sizes, i.e., small Au particles as co-catalysts for H₂ formation and large Au particles for

photoabsorption and oxidation. Here we report 1) precise control of Au particle distribution by the MS photodeposition method, 2) factors controlling properties and photocatalytic activity of Au/TiO₂ samples and 3) function of Au as a co-catalyst.

2. Experimental

2.1 Synthesis of nanocrystalline TiO₂

Nanocrystalline TiO₂ powder was prepared using the HyCOM (hydrothermal crystallization in organic media) method at 573 K. ¹² Titanium(IV) butoxide and toluene were used as the starting material and solvent, respectively. The product was calcined at 723 K for 1 h in a box furnace. The crystallinity of HyCOM-TiO₂ samples was improved by calcination, and the samples still had a large specific surface area of 97 m²g⁻¹ even after calcination at 723 K. Hereafter, calcined a HyCOM-TiO₂ sample is designated as TiO₂(calcination temperature), for example, a sample calcined at 723 K is shown as TiO₂(723).

2.2 Preparation of Au/TiO₂

Loading of Au on TiO₂ was performed by a photodeposition method. Bare TiO₂ powder (198 mg) was suspended in 10 cm³ of an aqueous solutions of methanol (50 vol%) in a test tube and the test tube was sealed with a rubber septum under argon (Ar). An aqueous solution of tetrachloroauric acid (HAuCl₄) was injected into the sealed test tube and then photoirradiated at $\lambda > 300$ nm by a 400-W high-pressure mercury arc (Eiko-sha, Osaka, Japan) under Ar with magnetic stirring in a water bath continuously kept at 298 K. The Au source was reduced by photogenerated electrons in the conduction band of TiO₂, and Au metal was deposited on TiO₂ particles, resulting in the formation of Au/TiO₂. Analysis of the liquid phase after each photodeposition revealed that the Au source had been almost completely (>99.9%) deposited as Au on the TiO₂ particles. The resultant powder was washed repeatedly with distilled water and then dried at 310 K overnight under air. In the MS photodeposition method, photodeposition of Au was repeated several times to obtain an Au/TiO₂ sample having a desired Au content. Hereafter, a sample prepared by the MS photodeposition method is designated as Au(X×Y)/TiO₂, where X and Y mean the amount of Au in wt% per photodeposition and the number of photodepositions, respectively. For example, Au(0.25×4)/TiO₂ was prepared by repeating 0.25 wt% photodeposition four times. In this study, the total amount of Au was fixed at 1.0 wt% (X×Y = 1.0).

2.3 Characterization

Diffuse reflectance spectra of Au/TiO₂ samples were obtained with a UV-visible spectrometer (UV-2400, Shimadzu, Kyoto) equipped with a diffuse reflectance measurement unit (ISR-2000, Shimadzu). The morphology of Au/TiO₂ samples was observed under a JEOL JEM-3010 transmission electron microscope (TEM) operated at 300 kV in the Joint Research Center of Kinki University. Spectra and light intensity of the Xe lamp (filtered) were determined using a spectroradiometer USR-45D (Ushio, Tokyo).

2.4 Photocatalytic activity test

2.4.1 H₂ formation from 2-propanol in aqueous suspensions of Au/TiO₂ under irradiation of visible light

Dried photocatalyst powder (50 mg) was suspended in 50 vol% 2-propanol-water solution (5 cm³), bubbled with Ar, and sealed with a rubber septum. The suspension was irradiated with visible light of a 500 W xenon (Xe) lamp (Ushio, Tokyo) filtered with a Y-48 filter (AGC Techno Glass) (450-600 nm: 83 mW cm⁻²) with magnetic stirring in a water bath continuously kept at 298 K. The amount of H₂ in the gas phase was measured using a Shimadzu GC-8A gas chromatograph equipped with an MS-5A column. The amount of acetone in the liquid phase was determined with a Shimadzu GC-14A gas chromatograph equipped with a fused silica capillary column (HiCap-CBP20, 25 m, 0.22 mm). Toluene was used as an internal standard sample. The reaction solution (1 cm³) was added to a diethyl ether/water mixture (2:1 v/v, 3 cm³). After the mixture had been stirred for 10 min, acetone in the ether phase was analyzed. The amount of acetone was determined from the ratio of the peak area of acetone to the peak area of toluene. In some experiments, another Xe lamp (LA-410UV, Hayashi Watch Works, Tokyo) was also used to evaluate activity of H₂ formation under irradiation of visible light coming from a light source other than the above Xe lamp.

2.4.2 Mineralization of acetic acid in aqueous suspensions of Au/TiO₂ under irradiation of visible light

Dried Au/TiO₂ powder (50 mg) was suspended in distilled water (5 cm³) in a test tube. The aqueous mixture was bubbled with oxygen (O₂) and the test tube was sealed with a rubber septum. Acetic acid (50 μ mol) was injected into the suspension and then irradiated with visible light from the 500 W Xe lamp (Ushio) with a Y-48 filter with magnetic stirring in a water bath continuously kept at 298 K. The amount of carbon dioxide (CO₂) in the gas phase of the reaction mixture was measured using a gas chromatograph (GC-8A, Shimadzu) equipped with a Porapak QS column.

2.4.3 H₂ formation from ammonia in aqueous suspensions of Au/TiO₂ under irradiation of visible light

Dried photocatalyst powder (50 mg) was suspended in an aqueous solution (5 cm³) containing ammonia (NH₃, 20 μ mol) in a test tube, bubbled with Ar, and sealed with a rubber septum. The suspension was irradiated with visible light of the 500 W Xe lamp (Ushio) filtered with a Y-48 filter with magnetic stirring in a water bath continuously kept at 298 K. The amounts of H₂ and nitrogen (N₂) in the gas phase were measured using a Shimadzu GC-8A gas chromatograph equipped with an MS-5A column.

3. Results and Discussion

3.1 Characterization of Au/TiO₂

Figure 1 shows TEM photographs of Au(1.0×1)/TiO₂(723) and Au(0.25×4)/TiO₂(723). Small Au particles were observed in the TEM photograph of Au(1.0×1)/TiO₂(723) and the average diameter of Au particles was determined to be 1.2 nm, suggesting that the one-step photodeposition can be used to highly disperse Au nanoparticles on the surface of TiO₂. On the other hand, two types of Au particles having different sizes were observed in the TEM photographs of Au(0.25×4)/TiO₂(723), although the number of larger particles was less than that of smaller particles. The average particle sizes of Au(0.25×4)/TiO₂(723) were determined to be 1.4 nm and 13 nm, respectively.

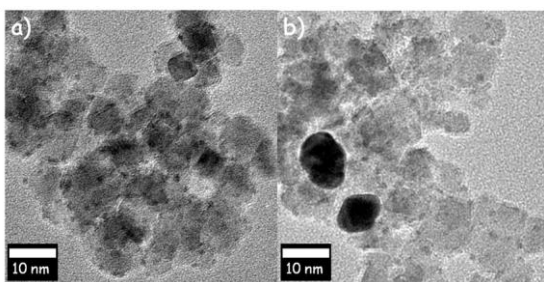


Figure 1 TEM images of (a) Au(1.0x1)/TiO₂(723) and (b) Au(0.25x4)/TiO₂(723) samples.

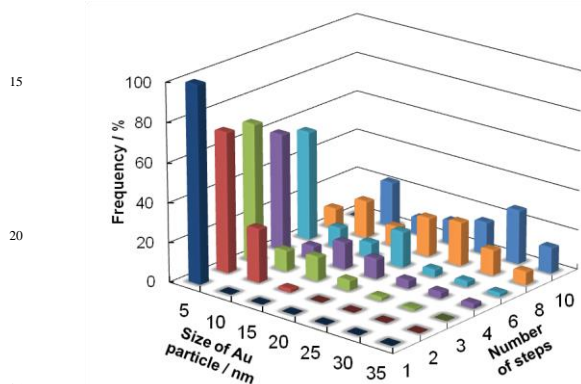


Figure 2 Effect of number of steps (Y) on distribution of Au nanoparticles of Au(XxY)/TiO₂(723) samples (XxY=1.0) prepared by the MS method.

These results indicate that the Au sources added after the first photodeposition were deposited on Au particles previously formed on the TiO₂ surface, resulting in growth of the Au particles, and that distribution of Au particles can be controlled by Y. The effect of Y on distribution of Au nanoparticles of Au/TiO₂(723) samples having 1.0 wt% Au was examined in detail by changing Y from 1 to 10, and the results are shown in Figure 2, in which X was simply determined by Y (X = 1.0/Y). The distribution of Au nanoparticles of Au/TiO₂(723) samples changed depending on Y, although the amounts of Au loaded on TiO₂ were the same (1.0 wt%). The proportion of smaller Au particles (< 5 nm) decreased with increase in Y, while the proportion of larger Au particles (> 10 nm) increased. Finally, smaller Au nanoparticles were not observed in Au(0.1x10)/TiO₂(723).

Absorption spectra of Au(1.0x1)/TiO₂(723) and Au(0.25x4)/TiO₂(723) are shown in Figure S1.^{11e} Photoabsorption was observed at 550 nm, which was attributed to SPR of the supported Au particles.^{8, 9, 10} It should be noted that Au(0.25x4)/TiO₂(723) exhibited much stronger photoabsorption than that of Au(1.0x1)/TiO₂(723), although the amounts of Au loaded on TiO₂ were the same. Figure 3(a) shows the intensities of photoabsorption at 550 nm of various Au/TiO₂(723) samples having 1.0 wt% Au. The intensity of photoabsorption of the samples increased with increase in Y up to Y=4 and tended to be saturated at Y>4. This result suggests that the intensity of photoabsorption due to SPR of Au was affected by the size of Au nanoparticles. Similar results have been obtained for plasmonic Au/TiO₂^{11e} and Au/CeO₂^{11f} photocatalysts and for unsupported

Au nanoparticles.¹³ In the last case, Shimizu *et al.*¹³ reported that such observed features coincide with prediction of the Mie theory.

3.2 Effect of the number of photodepositions on photocatalytic H₂ formation

Various 1.0 wt% Au/TiO₂(723) samples prepared by changing Y from 1 to 10 were used for formation of H₂ from 2-propanol in their aqueous suspensions under visible light irradiation from a Xe lamp with a Y-48 filter at 298 K. Just after irradiation of visible light, H₂ was evolved and formation of H₂ continued almost linearly with irradiation time, indicating that the 1.0 wt% Au/TiO₂(723) samples were active for H₂ formation. Rates of H₂ evolution are shown in Figure 3(b). The reaction rate increased until Y=6 and the rates of H₂ evolution at Y=1 and 6 were determined to be 0.15 and 3.1 μmol h⁻¹, respectively, i.e., the Au(0.17x6)/TiO₂(723) sample exhibited a rate of H₂ evolution that was ca. 21-times larger than that of the (1.0x1)Au/TiO₂(723) sample, even though the Au contents were the same. Intensity of SPR absorption seems to be one of the factors controlling the activity for H₂ production. However, the rates of H₂ evolution decreased at Y=8 and 10 even though the light intensities of the samples were the same (Figure 3(a)). Therefore, this tendency suggests that the presence of smaller Au nanoparticles as reduction sites was important as well as strong SPR absorption for H₂ evolution over Au/TiO₂(723) samples.

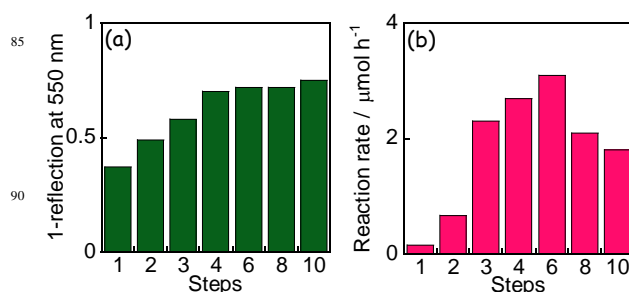


Figure 3 Effects of number of steps (Y) of Au(XxY)/TiO₂(723) samples (XxY=1.0) on (a) "1-reflection" at 550 nm and (b) rate of H₂ evolution from 2-propanol in aqueous suspensions under irradiation of visible light from a Xe lamp with a Y-48 filter.

3.3 Effect of post-calcination

Post-calcination has been widely applied to control the particle size of Au loaded on various supports. Akita *et al.*¹⁴ reported that the average size of small Au particles (~2 nm) in Au/TiO₂ increased with an increase in calcination temperature (> 473 K) and that the small particles disappeared at a temperature > 573 K. When Au(0.25x4)/TiO₂(723) was calcined at 773 K in air, smaller Au particles having an average diameter of 1.4 nm disappeared (Figure S2), suggesting that these smaller particles were unified with larger Au particles.^{11e} Figure 4 shows the effect of post-calcination temperature on the distribution of Au nanoparticles. It can be clearly seen that the proportion of smaller Au particles (< 5 nm) decreased with increase in post-calcination temperature and that Au particles on TiO₂ gradually grew with calcination. The effect of post-calcination temperature on photoabsorption of Au/TiO₂ samples at 550 nm is shown in Figure 5(a).

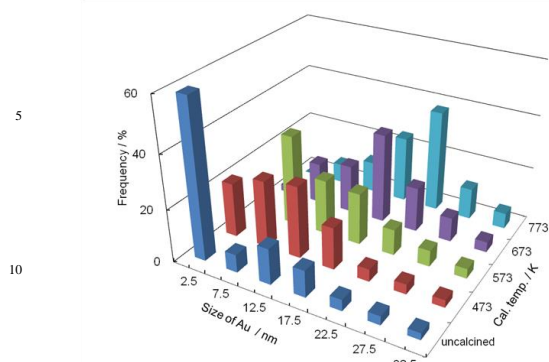


Figure 4 Change in distribution of Au particles by post-calcination of Au(0.25×4)/TiO₂(723).

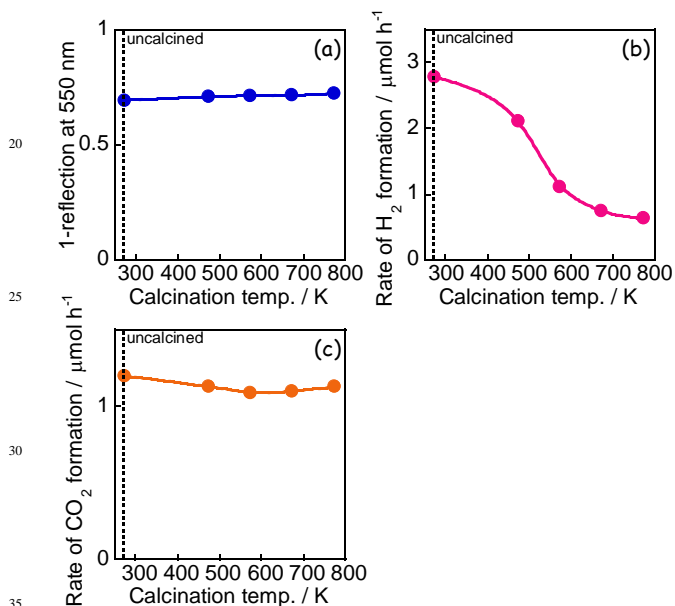


Figure 5 Effects of post-calcination temperature on (a) “1-reflection” at 550 nm of Au(0.25×4)/TiO₂(723), (b) rate of H₂ evolution from 2-propanol, and (c) rate of CO₂ formation from acetic acid in the presence of O₂.

Interestingly, calcination of the Au(0.25×4)/TiO₂(723) sample had almost no effect on in SPR, probably because the further increase in particle size had little effect on SPR of the sample before calcination. Totally, post-calcination of the Au(0.25×4)/TiO₂(723) sample had an effect on smaller Au particles (< 5 nm) not but on SPR intensity. Therefore, the role of smaller Au particles (< 5 nm) in H₂ evolution under irradiation of visible light was investigated by using Au(0.25×4)/TiO₂(723) and samples obtained by calcination of Au(0.25×4)/TiO₂(723) at various temperatures. Figure 5(b) shows the effect of post-calcination temperature on the rate of H₂ evolution from 2-propanol in aqueous suspensions of these samples. The rate of H₂ formation decreased with increase in post-calcination temperature, although the Au contents and SPR intensities of these samples were almost the same. These results suggest that smaller Au particles formed on TiO₂ by using the MS photodeposition method played important roles such as charge separation, electron storage and H⁺ reduction, not but photoabsorption, in H₂

formation under irradiation of visible light.

Photocatalytic reaction in the presence of O₂, i.e., photocatalytic mineralization, does not require a co-catalyst because O₂ is a good electron acceptor and one-electron reduction of O₂ by electrons in the conduction band of TiO₂ is possible without the aid of a co-catalyst. Therefore, Au(0.25×4)/TiO₂(723) and samples obtained by calcination of Au(0.25×4)/TiO₂(723) at various temperatures were used for mineralization of acetic acid in aqueous suspensions in the presence of O₂ under irradiation of visible light, and the effect of post-calcination on rate of CO₂ formation is shown in Figure 5(c). The rates of CO₂ formation were almost the same regardless of the temperature of post-calcination in contrast to the rates of H₂ formation (Figure 5(b)). The different temperature dependency of CO₂ formation indicates that the smaller Au nanoparticles had little effect on mineralization of acetic acid in the presence of O₂. Two different dependencies support the idea that smaller Au particles formed on TiO₂ work as a co-catalyst rather than the main photocatalyst in H₂ evolution, i.e., smaller Au particles have key roles in charge separation, electron storage and H⁺ reduction rather than photoabsorption, electron injection and substrate oxidation.

3.4 Effect of pre-calcination temperature

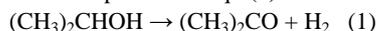
To examine the effects of physical properties and crystal structure, HyCOM-TiO₂ samples calcined at various temperatures (Z) [Z = 723-1273 K] were used as supports for Au particles. With elevation in calcination temperature, S_{BET} of TiO₂ gradually decreased. By using the MS photodeposition method, 1.0 wt% Au particles were loaded on TiO₂(Z), and Au(1.0×1)/TiO₂(Z) and Au(0.25×4)/TiO₂(Z) samples were prepared. These samples were used for H₂ evolution from 2-propanol under irradiation of visible light. Table 1 shows the yields of H₂ in the gas phase and acetone in the liquid phase after 10 h of irradiation as well as specific surface area of TiO₂, the crystalline phase of TiO₂, intensity of photoabsorption at 550 nm due to SPR, and average sizes of smaller and larger Au particles. In the series of Au(1.0×1)/TiO₂(Z) samples, only smaller Au particles were observed and the average size of the smaller Au particles increased with elevation in calcination temperature. The increase in particle size can be explained by the decrease in S_{BET} of TiO₂ with calcination, i.e., dispersion of Au on TiO₂ became worse with decrease in S_{BET} of TiO₂. Intensity of photoabsorption due to SPR increased with elevation in calcination temperature, though the Au contents were the same (1.0 wt%). These results indicate that photoabsorption due to SPR can be easily controlled by calcination temperature of TiO₂ before Au photodeposition. In all the of Au(0.25×4)/TiO₂(Z) samples, bimodal distributions of Au particles were observed. The average size of smaller Au particles increased with decrease in S_{BET} of TiO₂ as in the case of Au(1.0×1)/TiO₂(Z) samples, while the average sizes of larger Au particles were almost the same. Photoabsorption intensities at 550 nm of the Au(0.25×4)/TiO₂(Z) samples were almost the same regardless of the calcination temperature and average size of the smaller Au particles in contrast to the Au(1.0×1)/TiO₂(Z) samples. The behavior of the Au(0.25×4)/TiO₂(Z) samples indicates that the photoabsorption of Au(0.25×4)/TiO₂(Z) samples was determined by the larger Au particles in the range of 13-15 nm.

Table 1 Specific surface areas and crystal structures of various of TiO₂ samples and H₂ evolution from 2-propanol in aqueous suspensions of Au/TiO₂ under irradiation of visible light.^a

Z / K	^b S _{BET} / m ² g ⁻¹	^c Crystal structure	Au(1.0×1)/TiO ₂ (Z)					Au(0.25×4)/TiO ₂ (Z)				
			^d D _{Au} (smaller / larger)	^e 1-R	^f Y(H ₂) / μmol	^g Y(Ac) / μmol	Y(H ₂)/Y(Ac)	^d D _{Au} (smaller / larger)	^e 1-R	^f Y(H ₂) / μmol	^g Y(Ac) / μmol	Y(H ₂)/Y(Ac)
723	97	A	1.2/-	0.39	1.5	1.5	1.0	1.4/13	0.70	28	29	0.97
823	91	A	1.4/-	0.40	2.3	2.4	0.96	1.5/13	0.70	27	26	1.0
973	54	A	2.5/-	0.42	4.1	4.2	0.98	2.8/14	0.71	24	23	1.0
1073	31	A	3.6/-	0.45	8.6	7.8	1.1	3.8/14	0.72	20	22	0.91
1173	13	A, R	4.2/-	0.48	2.4	2.3	1.0	4.5/14	0.73	5.6	5.7	0.98
1273	2.3	R	5.5/-	0.55	trace	trace	-	5.6/15	0.72	trace	trace	-

^aTiO₂ was synthesized by the HyCOM method and calcined at Z K shown in parenthesis. ^bBET surface area. ^cA: anatase, R: rutile. ^dD_{Au}: average size of Au nanoparticles in Au/TiO₂. ^ePhotoabsorption at 550 nm due to SPR. ^fH₂ yield for 10 h. ^gAcetone yield for 10 h. ^f50 mg of photocatalyst and visible light in the range of 450-600 nm (83 mW cm⁻²).

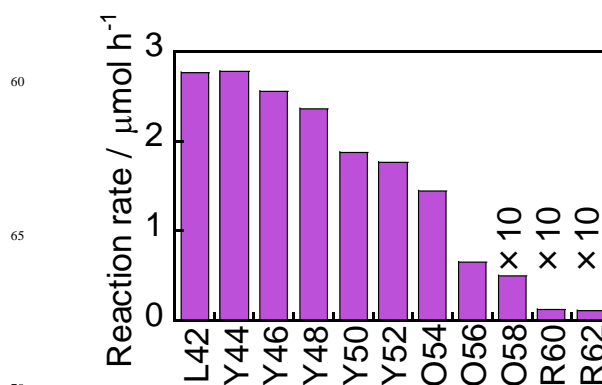
H₂ and acetone were formed in all anatase-type TiO₂ and anatase-rutile-mixed TiO₂ samples, whereas H₂ evolution from rutile-type TiO₂ samples was negligible. Since the conduction band of rutile-type TiO₂ is lower than that of anatase-type TiO₂, the position of the conduction band of the TiO₂ support seems to be important for Au/TiO₂ in H₂ evolution under the present reaction conditions. In case of the Au(1.0×1)/TiO₂(Z) samples, H₂ yield for 10 h reached a maximum (8.6 μmol) at Z = 1073 and further elevation in calcination temperature led to a gradual decrease in the photocatalytic activity. The yield of H₂ seems to be determined complexly depending on S_{BET}, crystal structure, particle size and photoabsorption due to SPR. On the other hand, the temperature dependency of the rate of Au(0.25×4)/TiO₂(Z) samples was simple. The Au(0.25×4)/TiO₂(723) sample exhibited the largest H₂ yield (28 μmol) probably because the largest S_{BET} and the smallest average size of Au particles contributed to adsorption of a large amount of 2-propanol and efficient H₂ evolution on the smaller Au particles, respectively. The ratios of the amount of H₂ formation to the amount of acetone over various Au(X×Y)/TiO₂(Z) samples are also shown in Table 1. Values around unity were obtained in all samples except rutile-type TiO₂ (Z = 1273 K). Good agreement with yields of H₂ and acetone in these samples shows that stoichiometric dehydrogenation of 2-propanol occurred as expressed in eqn (1).



As also clearly shown in Table 1, H₂ yields of the Au(0.25×4)/TiO₂(Z) samples were 2-19-times higher than those of the Au(1.0×1)/TiO₂(Z) samples. Since various factors intricately affect properties and functions of Au particles and final properties of Au/TiO₂, it is generally difficult to prepare an Au/TiO₂ sample satisfying all properties as a plasmonic photocatalyst by using a usual photodeposition method (Y = 1). The results of this study indicate that an Au/TiO₂ sample with an excellent property as a plasmonic photocatalyst can be easily prepared by using the MS photodeposition method.

3.5 Effect of cut-off filters

Figure 6 shows the effect of cut-off filters set in the Xe lamp on H₂ evolution from 2-propanol in aqueous suspensions of Au(0.25×4)/TiO₂(723). Figure 6 is different from an ordinary action spectrum, and the results indicate both the effects of wavelength of light and the amount of photons. The rate of H₂ formation decreased with increase in the filter number, corresponding to the decrease in photoabsorption. Especially, large decrease in the rate was observed when O58 cut-off filter was used. In the case of Au/cerium(IV) oxide, photoabsorption in the range of 600-700 nm mainly due to light scattering scarcely contributed to photocatalytic reaction.^{11c} Similarly, the large decrease in the rate observed in the Au(0.25×4)/TiO₂(723) sample is explained by the same reason.

**Figure 6** Effect of cut-off filters set in the Xe lamp on H₂ evolution from 2-propanol in an aqueous suspensions of Au(0.25×4)/TiO₂(723).

3.6 Effect of light intensity

Au(1.0×1)/TiO₂(723) and Au(0.25×4)/TiO₂(723) samples were used for H₂ formation from 2-propanol in aqueous suspensions under irradiation by light from a Xe lamp with a Y-44 filter with various light intensities (3.2-46 mW cm⁻²) as shown in Figure 7(a). Figure 7(b) shows the effect of light intensity on the rate of

H₂ formation. The rates increased with increase in light intensity in both samples, and the rates of Au(0.25×4)/TiO₂(723) were always larger than those of Au(1.0×1)/TiO₂(723). We noted that light intensity had different effects on the rate of H₂ formation over the two samples. The ratio of the rates of H₂ formation over the two samples (R4/R1) is shown in Figure 7(c). The value of R4/R1 decreased with increase in light intensity, which was due to the decrease in efficiency of Au(0.25×4)/TiO₂(723) (Figure 7(b)). Decrease in efficiency of photocatalytic reactions under irradiation of intense light is often observed in semiconductor photocatalysts and is generally explained by increased electron-hole recombination probability. Similarly, the decrease in the rates of Au(0.25×4)/TiO₂(723) under irradiation of intense light is explained by the same reason. In other words, excellence of Au(0.25×4)/TiO₂(723) is pronounced under irradiation of weaker light.

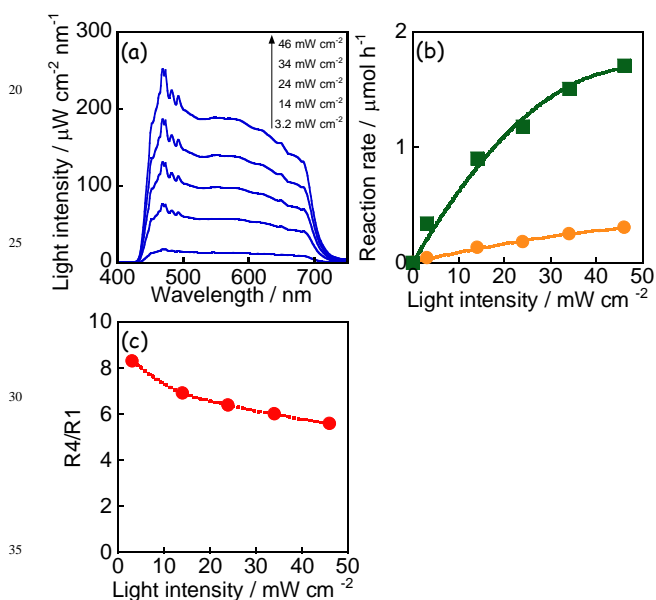


Figure 7 (a) Intensity of visible light irradiated to reaction systems from a Xe lamp with a Y-44 cut-off filter and effect of light intensity on (b) rate of H₂ formation from 2-propanol in aqueous suspensions of Au(1.0×1)/TiO₂(723) (circles) and Au(0.25×4)/TiO₂(723) (squares) and (c) ratio of the rates.

3.7 H₂ formation from NH₃

To extend the possibility of Au/TiO₂ for H₂ formation under visible light, NH₃ as biomass waste in water was used as a substrate. Figure 8 shows time courses of the evolution of H₂ and N₂ from NH₃ in an aqueous suspension of Au(0.25×4)/TiO₂(723) under irradiation of visible light. Since H₂ and N₂ increased linearly with photoirradiation time, the rates of H₂ and N₂ evolution were determined to be 0.84 and 0.29 μmol h⁻¹, respectively. After photoirradiation for 35 h, H₂ and N₂ evolution was almost saturated at around 30 and 10 μmol (H₂/N₂ ratio of 3.0), which corresponded to the initial amount of NH₃ (20 μmol), indicating that NH₃ was almost completely decomposed to H₂ and N₂ (eqn. (2)) over Au(0.25×4)/TiO₂(723) under irradiation of visible light.

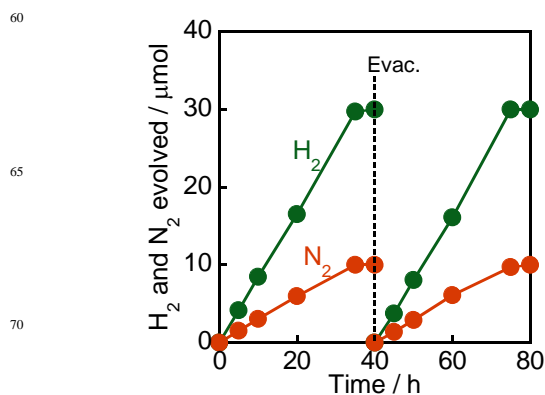
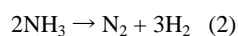


Figure 8 Time courses of evolution of H₂ and N₂ from NH₃ in an aqueous suspension of Au(0.25×4)/TiO₂(723) under irradiation of visible light from a Xe lamp with a Y-48 filter. After 40-h irradiation and evacuation, additional NH₃ (20 μmol) was injected and the suspension was irradiated again.

To evaluate the stability of Au/TiO₂ in H₂ and N₂ production from NH₃, Au(0.25×4)/TiO₂(723) was used again. Irradiation of visible light to the reaction mixtures again induced evolution of H₂ and N₂, and the formation continued from 40 h to 80 h without deactivation.

Conclusions

Gold (Au)-loaded titanium(IV) oxide (Au/TiO₂) having both smaller and larger Au particles was successfully prepared by the multi-step (MS) photodeposition method. Au particle distribution and photoabsorption properties of Au/TiO₂ can be controlled by conditions of the MS photodeposition, post-calcination of Au/TiO₂ and properties of TiO₂ before Au loading. In hydrogen (H₂) formation from 2-propanol in aqueous suspensions of Au/TiO₂ under irradiation of visible light, co-existence of large (>10 nm) and small (<5 nm) Au particles was indispensable for higher activities, which contributed to strong photoabsorption due to surface plasmon resonance (SPR) and efficient H₂ evolution (proton reduction), respectively. Au/TiO₂ having a bimodal Au distribution can be applied for stoichiometric decomposition of ammonia to H₂ and nitrogen under visible light irradiation. On the other hand, in the case of mineralization of acetic acid in the presence of oxygen (O₂), small Au particles are not requisite because O₂ is a good electron acceptor and one-electron reduction of O₂ by electrons in the conduction band of TiO₂ is possible without the aid of a co-catalyst. These results suggest that separate loading of co-catalyst particles without alloying with Au particles is effective for enhancing activities of an Au plasmonic photocatalyst in reactions in which reaction rates are controlled by electron consumption.

Acknowledgements

This work was partly supported by a Grant-in-Aid for Scientific Research (No. 23560935) from the Ministry of Education, Culture, Sports, Science, and Technology (MEXT) of Japan. The authors (H. K. and A. T.) are grateful for financial support from Iketani Science and Technology Foundation. One of

the authors (A. T.) appreciates the Japan Society for the Promotion of Science (JSPS) for a Research Fellowship for Young Scientists.

Notes and references

⁵ Department of Applied Chemistry, Faculty of Science and Engineering, Kinki University, Kowakae, Higashiosaka, Osaka 577-8502, Japan; E-mail: hiro@apch.kindai.ac.jp

† Electronic Supplementary Information (ESI) available: Figure S1 and Figure S2. See DOI: 10.1039/b000000x/

- 1 (a) M. A. Fox, M. T. Dulay, *Chem. Rev.*, 1993, **93**, 341; (b) M. R. Hoffmann, S. T. Martin, W. Choi, D. W. Bahnemann, *Chem. Rev.*, 1995, **95**, 69.
- 2 (a) F. Mahdavi, T. C. Bruton, Y. Li, *J. Org. Chem.*, 1993, **58**, 744; (b) J. L. Ferry, W. H. Glaze, *Langmuir*, 1998, **14**, 3551; (c) K. Imamura, K. Hashimoto, H. Kominami, *Chem. Commun.*, 2012, **48**, 4356; (d) H. Tada, T. Ishida, A. Takao, S. Ito, *Langmuir*, 2004, **20**, 7898; (e) Y. Shiraishi, Y. Togawa, D. Tsukamoto, S. Tanaka, T. Hirai, *ACS Catal.*, 2012, **2**, 2475-2481; (f) K. Fuku, K. Hashimoto, H. Kominami, *Chem. Commun.*, 2010, **46**, 5118; (g) K. Fuku, K. Hashimoto, H. Kominami, *Catal. Sci. Technol.*, 2011, **1**, 586.
- 3 (a) T. Kawai, T. Sakata, *Nature*, 1980, **286**, 474; (b) K. Shimura, H. Yoshida, *Energy Environ. Sci.*, 2011, **4**, 2467; (c) H. Kominami, H. Nishimune, Y. Ohta, Y. Arakawa, T. Inaba, *Appl. Catal. B*, 2012, **111-112**, 297; (d) H. Yuzawa, T. Mori, H. Itoh, H. Yoshida, *J. Phys. Chem. C*, 2012, **116**, 4126.
- 4 R. Asahi, T. Morikawa, T. Ohwaki, K. Aoki, Y. Taga, *Science*, 2001, **293**, 269.
- 5 T. Ohno, M. Akiyoshi, T. Umebayashi, K. Asai, T. Mitui, M. Matsumura, *Appl. Catal. A*, 2004, **265**, 115.
- 6 H. Irie, S. Miura, K. Kamiya, K. Hashimoto, *Chem. Phys. Lett.*, 2008, **457**, 202.
- 7 (a) H. Kisch, L. Zang, C. Lange, W. F. Maier, C. Antonius, D. Meissner, *Angew. Chem. Int. Ed. Engl.*, 1998, **37**, 3034; (b) H. Kominami, K. Sumida, K. Yamamoto, N. Kondo, K. Hashimoto, Y. Kera, *Res. Chem. Intermed.*, 2008, **34**, 587; (c) S. Kitano, K. Hashimoto, H. Kominami, *Appl. Catal. B: Environ.*, 2011, **101**, 206; (d) S. Kitano, N. Murakami, T. Ohno, Y. Mitani, Y. Nosaka, H. Asakura, K. Teramura, T. Tanaka, H. Tada, K. Hashimoto, H. Kominami, *J. Phys. Chem. C*, 2013, **117**, 11008.
- 8 (a) X. Chen, S. Shen, L. Guo, S. S. Mao, *Chem. Rev.*, 2010, **110**, 6503; (b) R. M. Navarro, M. C. Sa´nchez-Sa´nchez, M. C. Alvarez-Galvan, F. del Valle, J. L. G. Fierro, *Energy Environ. Sci.* 2009, **2**, 35.
- 9 (a) M. Xiao, R. Jiang, F. Wang, C. Fang, J. Wang, J. C. Yu, *J. Mater. Chem. A*, 2013, **1**, 5790; (b) S. C. Warren, E. Thimsen, *Energy Environ. Sci.*, 2012, **5**, 5133; (c) X. Zhou, G. Liu, J. Yu, W. Fan, *J. Mater. Chem.*, 2012, **22**, 21337; (d) S. Linic, P. Christopher, D. B. Ingram, *Nature Mater.*, 2011, **10**, 911.
- 10 (a) Y. Tian and T. Tatsuma, *J. Am. Chem. Soc.*, 2005, **127**, 7632; (b) A. Furrube, L. Du, K. Hara, R. Katoh and M. Tachiya, *J. Am. Chem. Soc.*, 2007, **129**, 14852; (c) S. Naya, M. Teranishi, T. Isobe and H. Tada, *Chem. Commun.*, 2010, **46**, 815; (d) E. Kowalska, R. Abe and B. Ohtani, *Chem. Commun.*, 2009, 241; (e) E. Kowalska, O. O. P. Mahaney, R. Abe and B. Ohtani, *Phys. Chem. Chem. Phys.*, 2010, **12**, 2344; (f) C. G. Silva, R. Juarez, T. Marino, R. Molinari, H. Garcia, *J. Am. Chem. Soc.*, 2011, **133**, 595; (g) H. Yuzawa, T. Yoshida, H. Yoshida, *Appl. Catal. B*, 2012, **115**, 294; (h) X. Ke, X. Zhang, J. Zhao, S. Sarina, J. Barry, H. Zhu, *Green Chem.*, 2013, **15**, 236.
- 11 (a) H. Kominami, A. Tanaka and K. Hashimoto, *Chem. Commun.*, 2010, **46**, 1287; (b) H. Kominami, A. Tanaka and K. Hashimoto, *Appl. Catal. A*, 2011, **397**, 121; (c) A. Tanaka, K. Hashimoto and H. Kominami, *ChemCatChem*, 2011, **3**, 1619; (d) A. Tanaka, K. Hashimoto and H. Kominami, *Chem. Commun.*, 2011, **47**, 10446; (e) A. Tanaka, S. Sakaguchi, K. Hashimoto and H. Kominami, *Catal. Sci. Technol.*, 2012, **2**, 907; (f) A. Tanaka, K. Hashimoto and H. Kominami, *J. Am. Chem. Soc.*, 2012, **134**, 14526; (g) A. Tanaka, A. Ogino, M. Iwaki, K. Hashimoto, A. Ohnuma, F. Amano, B. Ohtani, H. Kominami, *Langmuir*, 2012, **28**, 13105; (h) A. Tanaka, S. Sakaguchi, K. Hashimoto and H. Kominami, *ACS catal.*, 2013, **3**, 79; (i) A. Tanaka, K. Hashimoto, B. Ohtani, H. Kominami, *Chem. Commun.*, 2013, **49**, 3419-3421; (j) A. Tanaka, Y. Nishino, S. Sakaguchi, T. Yoshikawa, K. Imamura, K. Hashimoto, H. Kominami, *Chem. Commun.*, 2013, **49**, 2551; (k) A. Tanaka, K. Nakanishi, R. Hamada, K. Hashimoto, H. Kominami, *ACS Catal.*, 2013, **3**, 1886.
- 12 (a) Kominami, H.; Kohno, M.; Takada, Y.; Inoue, M.; Inui T.; Kera, Y. *Ind. Eng. Chem. Res.*, 1999, **38**, 3925; (b) Kominami, H.; Murakami, S.-y.; Kato, J.-i.; Kera, Y.; Ohtani, B. *J. Phys. Chem. B*, 2002, **106**, 10501.
- 13 T. Shimizu, T. Teranishi, S. Hasegawa, M. Miyake, *J. Phys. Chem. B*, 2003, **107**, 2719.
- 14 T. Akita, P. Lu, S. Ichikawa, K. Tanaka, M. Haruta, *Surf. Interface Anal.*, 2001, **31**, 73.